SUPPLEMENT ARTICLE

# Novel Small Molecule Entry Inhibitors of Ebola Virus

**Arnab Basu,[1] Debra M. Mills,[1] Daniel Mitchell,[2] Esther Ndungo,[3] John D. Williams,[1] Andrew S. Herbert,[4] John M. Dye,[4] Donald T. Moir,[1] Kartik Chandran,[3] Jean L. Patterson,[2] Lijun Rong,[5] and Terry L. Bowlin[1]**

[1]Microbiotix, Inc, Worcester, Massachusetts; [2]Texas Biomedical Research Institute, San Antonio; [3]Albert Einstein College of Medicine, Bronx, New York; [4]Army Medical Research Institute of Infectious Diseases, Frederick, Maryland; and [5]Department of Microbiology and Immunology, College of Medicine, University of Illinois at Chicago

***Background.*** The current Ebola virus (EBOV) outbreak has highlighted the troubling absence of available antivirals or vaccines to treat infected patients and stop the spread of EBOV. The EBOV glycoprotein (GP) plays critical roles in the early stage of virus infection, including receptor binding and membrane fusion, making it a potential target for the development of anti-EBOV drugs. We report the identification of 2 novel EBOV inhibitors targeting viral entry.

***Methods.*** To identify small molecule inhibitors of EBOV entry, we carried out a cell-based high-throughput screening using human immunodeficiency virus–based pseudotyped viruses expressing EBOV-GP. Two compounds were identified, and mechanism-of-action studies were performed using immunoflourescence, AlphaLISA, and enzymatic assays for cathepsin B inhibition.

***Results.*** We report the identification of 2 novel entry inhibitors. These inhibitors (1) inhibit EBOV infection (50% inhibitory concentration, approximately 0.28 and approximately 10 μmol/L) at a late stage of entry, (2) induce Niemann-Pick C phenotype, and (3) inhibit GP–Niemann-Pick C1 (NPC1) protein interaction.

***Conclusions.*** We have identified 2 novel EBOV inhibitors, MBX2254 and MBX2270, that can serve as starting points for the development of an anti-EBOV therapeutic agent. Our findings also highlight the importance of NPC1-GP interaction in EBOV entry and the attractiveness of NPC1 as an antifiloviral therapeutic target.

***Keywords.*** Ebola virus; Niemann-Pick C1; Ebola envelope glycoprotein; antiviral.

Zaire Ebola virus (EBOV) infection causes acute hemorrhagic fever in humans and nonhuman primates with mortality rate exceeding 50% in many outbreaks [1–3]. The World Health Organization has declared the current EBOV outbreak in West Africa as a public health emergency. Without an available vaccine or drug, the treatment for EBOV infection has been primarily limited to palliative care and barrier methods to prevent transmission. In addition, ZMapp and other experimental EBOV drugs have been administered to infected patients on a case-by-case "compassionate use" basis. These approaches, have currently slowed the EBOV outbreak [4]. The viral genome encodes 8 viral proteins: nucleoprotein (NP), VP35, VP40, EBOV glycoprotein (GP), soluble glycoprotein (sGP), VP30, VP24, and RNA-dependent RNA polymerase (L). EBOV-GP is the only viral envelope GP. Mature EBOV-GP is a homotrimer, and each monomer is composed of 2 disulfide-linked polypeptides, GP1 and GP2, generated by proteolytic cleavage of the primary translation product GP0 [5, 6].

Viral entry is the first and an essential step in the viral replication cycle. EBOV-GP mediates viral attachment and entry into cells. After attachment on susceptible cells, the viruses undergo endocytosis, probably through macropinocytosis, although additional endocytic pathways have been implicated. The internalized virus localizes in late endosomes/lysosomes (LE/LYs), whereby the cysteine proteases, primarily cathepsin B (CatB, cleave EBOV-GP to a 19-kDa fragment. The cleaved EBOV-GP serves a ligand for Niemann-Pick C1 (NPC1), a multimembrane spanning cholesterol transport protein in LE/LYs. EBOV-GP/NPC1 domain C interaction is essential for entry in target cells [7–9].

Correspondence: Arnab Basu, PhD, Microbiotix, Inc, 1 Innovation Dr, Worcester, MA 01605 (abasu@microbiotix.com).

**The Journal of Infectious Diseases® 2015;212:S425–34**

DOI: 10.1093/infdis/jiv223

Blocking viral entry into the target cell leads to suppression of viral infection and the accompanying cytokine storm and is therefore an attractive antiviral strategy [3, 5]. Basu et al [5] have reported elsewhere the establishment of a high-throughput screening assay for identification of EBOV entry inhibitors using pseudotype virus and an EBOV entry inhibitor with a benzodiazepine scaffold. In this report, we describe the identification and characterization of 2 novel entry inhibitors from a different high-throughput screening using pseudotype viruses. These inhibitors (1) inhibit EBOV infection (50% inhibitory concentrations [$IC_{50}$], approximately 0.28 and approximately 10 μmol/L) in vitro, (2) induce a Niemann–Pick type C phenotype in cells, and (3) inhibit EBOV-GP/NPC1 protein interaction. Our findings suggest that the EBOV-GP/NPC1 domain C interaction can be targeted to develop an anti-EBOV drug

## METHODS

### Cell Lines, Viruses, and Plasmids

The 293T, A549, and VeroE6 cell lines were procured from the American Type Culture Collection. Plasmid vectors expressing the wild type EBOV Zaire envelope protein (EBOV-GP; GenBank accession number L11365), EBOV-GP with deletion in mucin region (EBOVGPΔmucin), and vesicular stomatitis virus envelope glycoprotein (VSV-G) were used as described elsewhere [5, 10–12]. A recombinant vesicular stomatitis Indiana virus (rVSV-GPΔ), encoding the enhanced green fluorescent protein and the EBOV-GP from which the mucinlike domain had been genetically deleted (Δ309–489; Δmuc), was generated and used to infect Vero cells, following methods described elsewhere [13].

### Compounds

The chemical library screened represents a broad and well-balanced collection of approximately 106 000 compounds accumulated over a number of years from a variety of distinct sources and has been described elsewhere in detail [5, 10]. We also used EBOV entry inhibitors compound 7 and compounds 3.47 and E64, described elsewhere, as controls [5].

### Pseudotyping and High-Throughput Screening of Chemical Libraries

Pseudotype viruses expressing either EBOV-GP or VSV envelope protein (VSV-G) (human immunodeficiency virus [HIV]/VSV-G) and a luciferase reporter gene were generated by cotransfecting replication defective HIV vector (pNL4–3-Luc-R-E−) with either EBOV-GP or VSV-G into 293T cells, as described elsewhere [5, 10–12]. Deletions in the HIV genome make the pseudotypes replication deficient.

High-throughput screening of chemical libraries for EBOV entry inhibitors was performed using HIV/EBOV-GP and 293T cells (10 000 cells/well) in 96-well plates, as described elsewhere [5, 10]. The final concentration of test compounds and dimethyl sulfoxide (DMSO) were 25 μmol/L and 1%, respectively, in all wells. Infection was quantified from the luciferase activity of the infected cells using the Britelite Plus assay system (Perkin Elmer) in a Wallac EnVision 2102 Multilabel Reader (Perkin Elmer). In the DMSO control, the assay showed an average luciferase signal of $1.2 \times 10^6 \pm 0.6 \times 10^6$ relative luciferase unit (RLU), a signal-to-background ratio of $>10^3$, and a calculated screening window coefficient (Z′ factor) [14], of $>0.5 \pm 0.2$. The luciferase signal standard error was ±50%, and >90% inhibition of luciferase activity at 25 μmol/L concentration was used as the criterion for designating a compound as a "hit."

The $IC_{50}$ values of "hit" compounds on HIV/EBOV-GP were then measured in a dose-dependent manner. Simultaneously, the toxicity of the compounds was determined by measuring the Glyceraldehyde 3-phosphate dehydrogenase (GAPDH) level in cell lysate, using an AlphaScreen SureFire GAPDH Assay kit (Perkin Elmer), as described elsewhere [10].

### Infectious EBOV Experiments

All experiments with cell culture-grown infectious EBOV were performed under biosafety level 4 conditions at the Texas Biomedical Research Institute in San Antonio, Texas. Virus was preincubated with either MBX2254 (0.0001–10 μmol/L) or MBX2270 (0.5–50 μmol/L) for 1 hour at room temperature before infection. After preincubation the virus-compound mixture was used to infect Vero E6 cells (multiplicity of infection, 1). One hour after infection (37°C), fresh medium (2% fetal bovine serum) containing the compound at the same concentrations was applied, followed by incubation for 8 days at 37°C. The culture medium was collected and titrated on new Vero E6 cells to determine the inhibition of virus infection. The viral titer was determined by (1) first fixing and inactivating cells with 10% buffered formalin, (2) staining with crystal violet, and (3) counting plaques.

The toxicity of the compounds on VeroE6 cells was determined by applying CellMask Deep Red stain (H32721) to untreated and treated cells at 5 μg/mL for 30 minutes after the culture medium was removed for titration. Cells were then restained with Hoescht stain (1 μg/mL), and plates were imaged (200× magnification) using a Nikon Ti Eclipse epifluorescence microscope. Cells displaying both blue and red stain were counted as live cells.

### Time-of-Addition Experiment

The "time-of-addition" experiment was performed using A549 cells, as described elsewhere [5]. A549 cells were treated with MBX2254 (10 μmol/L) and MBX2270 (30 μmol/L) at −1, 0, 2 or 12 hours and infected with HIV/EBOV-GP. Cells were harvested after 48 hours to check for infection. Duplicate wells were used for each time point. Control infected cultures were treated with either DMSO (no inhibition) or E64, an EBOV entry inhibitor [5].

### Cholesterol Accumulation Assay

Cholesterol accumulation was monitored using filipin staining of A549 cells treated with MBX2254 (10 μmol/L) or MBX2270 (30 μmol/L), as described elsewhere [15, 16]. Cells were (1) plated on coverslips in a 24-well plate; (2) treated with MBX2254 (10 μmol/L), MBX2270 (30 μmol/L), E64 (0.1 μmol/L), or 3.47 (10 μmol/L) for 20 hours; (3) fixed with 10% formalin; (4) incubated with 50 μg/mL filipin (Sigma-Aldrich) for 1 hour at room temperature; and (4) imaged using a Nikon TE-2000E2 fluorescence microscope with a motorized Z drive.

### CatB Activity Assays and Endosomal Acidification

We used a fluorometric assay to measure CatB activity that uses an internally quenched fluorogenic peptide substrate, Z-Phe-Arg-7-amido-4-methylcoumarin hydrochloric acid (Calbiochem). CatB activity was measured in a dose-dependent manner in 96-well plates, as described elsewhere [17]. Cleavage of the substrate by CatB releases amido-4-methylcoumarin, and the fluorescence is measured at 360 nm excitation and 460 nm emission, and the readout is reported as RLU.

Endosomal acidification was assessed in A549 cells using Lysotracker Red (Molecular Probes) as a probe for low-pH organelles. Cells were pretreated with treated with MBX2254 (10 μmol/L), MBX2270 (30 μmol/L), E64 (0.1 μmol/L), or 3.47 (10 μmol/L) for 1 hour at 37°C and then incubated with 50 nmol/L Lysotracker Red for 30 minutes. Cells were then fixed and analyzed with fluorescence microscopy.

### AlphaLISA Assay to Measure EBOV-GP/NPC1 Interaction

We adapted the AlphaLISA format (Perkin-Elmer) to measure the EBOV-GP/NPC1 domain C interaction in a 384-well plate format. Cleaved EBOV-GP was first captured onto protein G–tagged AlphaLISA acceptor beads using the anti-EBOV-GP monoclonal antibody KZ52 [13, 18]. Anti-FLAG tagged donor beads were coated with FLAG-tagged NPC1 domain C peptide, as described elsewhere [13]. On mixing, EBOV-GP-NPC1 interaction brings the acceptor and donor beads into close proximity, allowing energy transfer from donor to acceptor bead, and inducing light emission at 520–620 nm. Fluorescence was measured using an AlphaLISA-compatible plate reader. The concentrations of each assay component, KZ52 capture antibody (39 ng/μL), EBOV-GP (18.8 ng/μL), and NPC1 domain C (18.8 ng/μL), were optimized.

## RESULTS

### MBX2254 and MBX2270 Inhibit EBOV Infection In Vitro

HIV/EBOV-GP contains an "HIV core" with a luciferase reporter gene and EBOV-GP on the viral surface [5]. The inhibitory effects of small molecules were quantified by measuring the decrease in the mean luciferase activity. Two compounds, MBX2254, a sulfonamide, and MBX2270, a triazole thioether (Figure 1*A* and 1*B*),

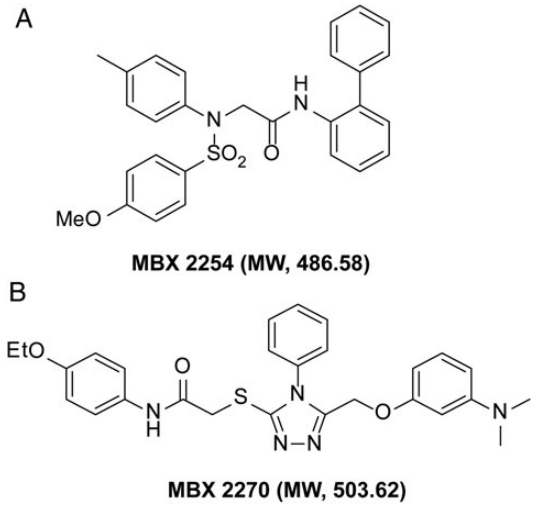


**Figure 1.** Chemical structure of MBX2254 and MBX2270, with molecular weight (MW). MBX2254 and MBX2270, with aminoacetamide sulfonamide and triazole thioether scaffolds, respectively, were prioritized based on chemical tractability (synthetically accessible, stable, druglike structures) and selectivity against Ebola pseudotype virus. Abbreviations: Eto, ethylene oxide; H, hydrogen; MeO, methoxy group; N, nitrogen, O, oxygen; $SO_2$, sulfur dioxide.

were identified from screening of chemically diverse small molecule libraries (106 440 compounds) with HIV/EBOV-GP, following methods described elsewhere [5, 10]. MBX2254 and MBX2270 displayed ≥90% reduction of the mean luciferase activity of the positive control [uninhibited HIV/EBOV-GP] at a test concentration of 25 μmol/L. These 2 hits were subsequently resynthesized and retested. The resynthesized compounds were determined to have the correct mass and to be >95% pure by liquid chromatography–mass spectrometry.

Both MBX2254 and MBX2270 displayed dose-dependent inhibition of HIV/EBOV-GP, with 90% inhibitory concentrations of 3 and 15.1 μmol/L, respectively (Figure 2*A* and 2*B*) and no significant toxicity up to 50 μmol/L (the maximum concentration tested). The specificity of the inhibition was evaluated by investigating the activity of MBX2254 and MBX2270 against HIV/VSV-G. Both MBX2254 and MBX2270 had no effect on HIV/VSV-G infectivity at a concentration of 25 μmol/L (data not shown).

Both MBX2254 and MBX2270 inhibited cell culture-grown infectious EBOV in a dose-dependent manner in cell culture. The $IC_{50}$ for MBX2254 and MBX2270 was determined to be 0.285 and 10 μmol/L, respectively, using Vero E6 cells (Figure 2*C* and 2*D*).

### MBX2254 and MBX2270 Inhibition of a Late Stage of EBOV Entry

Time-of-addition experiments were performed with HIV/EBOV-GP to determine the stages of EBOV entry blocked by MBX2254 and MBX2270. MBX2254 and MBX2270 were added 1 hour before infection (−1 hour), during infection (0 hour), and 2 and 12

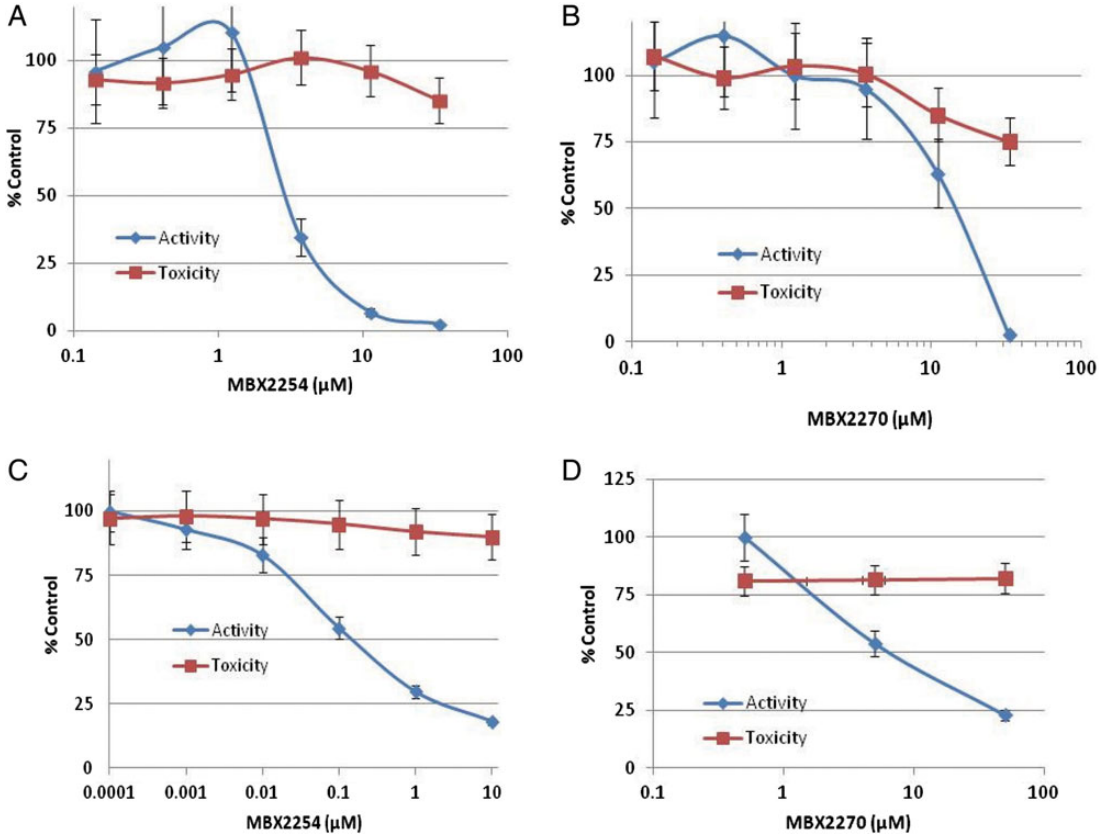


**Figure 2.** Effects of MBX2254 and MBX2270 on Ebola virus (EBOV) infection. The inhibitory effect of compounds MBX2254 and MBX2270 on Ebola pseudotype virus (HIV/EBOV-GP) (*A, B*) and infectious EBOV-Zaire (*C, D*). Dose-response curves for the MBX2254 and MBX2270 are shown. Infectivity was investigated as described in "Methods" section. A multiplicity of infection of 1.0 was used for infectious EBOV-Zaire. Three independent experiments were performed to determine the effects of compounds.

hours after infection (Figure 3*A*) at 10 and 30 μmolL, respectively, slightly above their 90% inhibitory concentration of 8.6 and 25.7 μmol/L respectively. Control infected cultures were treated with either DMSO (no inhibition) or E64 (0.02 μmol/L) an EBOV entry inhibitor [5]. MBX2254, MBX2270, and E64 inhibited >90% of HIV/EBOV-GP infection when added at −1, 0, or 2 hours, relative to virus infection (Figure 3*A*). Interestingly, when MBX2254 and MBX2270 were added 12 hours after the virus adsorption process at 37°C, inhibition was not observed.

We further investigated whether the compounds MBX2254 and MBX2270 act as receptor antagonists to inhibit HIV/EBOV-GP infection. A549 cells were pretreated for 1 hour with MBX2254 and MBX2270 at 0°C at 10 and 30 μmol/L respectively, followed by washing of the cells and subsequent adsorption of the HIV/EBOV-GP at 0°C. Control infected cultures were treated with either DMSO or E64 (0.02 μmol/L). No significant inhibition was observed after the pretreatment of cells (Figure 3*B*). These results suggest that, like E64, MBX2254 and MBX2270 act on a late stage during the virus entry process.

To further characterize the mechanism of action, we investigated the effect of MBX2254 and MBX2270 on CatB activity. Controls include either compound 7, a known entry inhibitor with no effect on CatB [5] or E64, a pancaspase inhibitor. MBX2254 and MBX2270 did not inhibit CatB activity levels, even at the maximum concentration tested (10 μmol/L) (Figure 3*C*).

Endosomal acidification was assessed in A549 cells with LysoTracker Red, a probe for low-pH organelles. Cells were treated with DMSO (vehicle), MBX2254 (10 μmol/L), MBX2270 (30 μmol/L), compound 3.47 (10 μmol/L), or ammonium chloride ($NH_4Cl$; 10 mmol/L). $NH_4Cl$ inhibits endosomal acidification and was used as a positive control. No inhibition was observed with either MBX2254 or MBX2270 (Figure 3*D*) whereas $NH_4Cl$ inhibited endosomal acidification (Figure 3*D*).

### MBX2254 and MBX2270 Disruption of the In Vitro Interaction of Primed EBOV-GP With NPC1

We next investigated the effects of the 2 inhibitors on cholesterol accumulation. Both MBX2254 (10 μmol/L) and MBX2270 (30 μmol/L) induced cholesterol accumulation in LE/LYs (Figure 4*A* and 4*B*). In contrast, E64 (0.1 μmol/L), a pancaspase inhibitor, did not cause detectable cholesterol accumulation

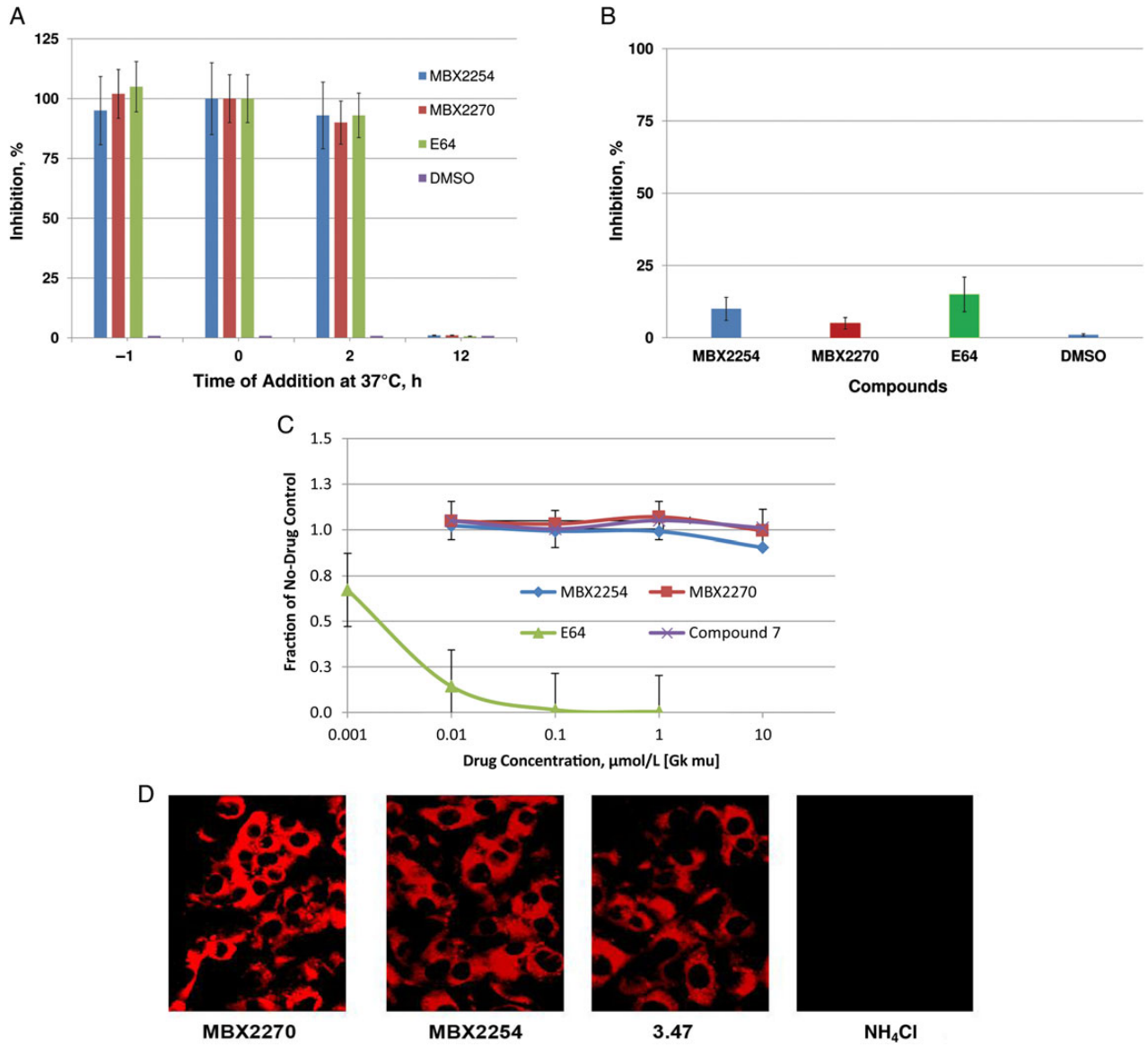


**Figure 3.** MBX2254 and MBX2270 inhibit a late stage of Ebola virus (EBOV) entry. *A*, Single-cycle time-of-addition experiment was performed with Ebola pseudotype virus (HIV/EBOV-GP) to determine the stage of EBOV entry blocked by MBX2254 and MBX2270, using A549 cells as described in "Methods" section. MBX2254 (10 µmol/L) and MBX2270 (30 µmol/L) were added for 1 hour before infection (−1 hour), 1 hour during adsorption (0 hour), and 2 hours and 12 hours after infection. Inhibition of HIV/EBOV-GP pseudotype infection was detected as a reduced luciferase signal. Error bars indicate standard deviations. *B*, MBX2254 and MBX2270 do not act as receptor antagonists. A549 cells were pretreated with MBX2254 (10 µmol/L) and MBX2270 (30 µmol/L) at 0°C for 1 hour. After incubation, the compounds were removed and cells were washed with ice-cold phosphate-buffered saline and infected with HIV/EBOV-GP at 0°C. After 1 hour of infection, unadsorbed viruses were washed with phosphate-buffered saline and incubated for 72 hours at 37°C. Inhibition of HIV/EBOV-GP pseudotype infection was detected as a reduced luciferase signal. Error bars indicate standard deviations. *C*, Inhibitory activity against cathepsin B (CatB) in vitro. MBX2254 and MBX2270 were evaluated, as described in "Methods" section, for their effects on CatB. E64, a pancaspase inhibitor, was included as a positive control for the assay. Compound 7, another EBOV entry inhibitor (reported elsewhere) that does not modulate CatB, was used as negative control. *D*, Endosomal pH on exposure to MBX2254 and MBX2270. A549 cells were preincubated in the presence of MBX2254 and MBX2270. After incubation, cells were fixed, stained with LysoTracker Red, and then viewed and photographed with a confocal microscope. Compound 3.47, a known EBOV entry inhibitor that does not modulate endosomal pH, was used as a negative control, and 10 mmol/L ammonium chloride ($NH_4Cl$) was used as a positive control for inhibition of acidification.

(Figure 4*D*). Compound 3.47 (10 µmol/L), which is reported to block binding of EBOV-GP to NPC1 [9], caused cholesterol accumulation in LE/LYs (Figure 4*C*).

NPC1 is involved in cholesterol transport. Binding of 19 kb cleaved EBOV-GP to the second luminal domain of NPC1; domain C is essential for EBOV entry [13]. We investigated the

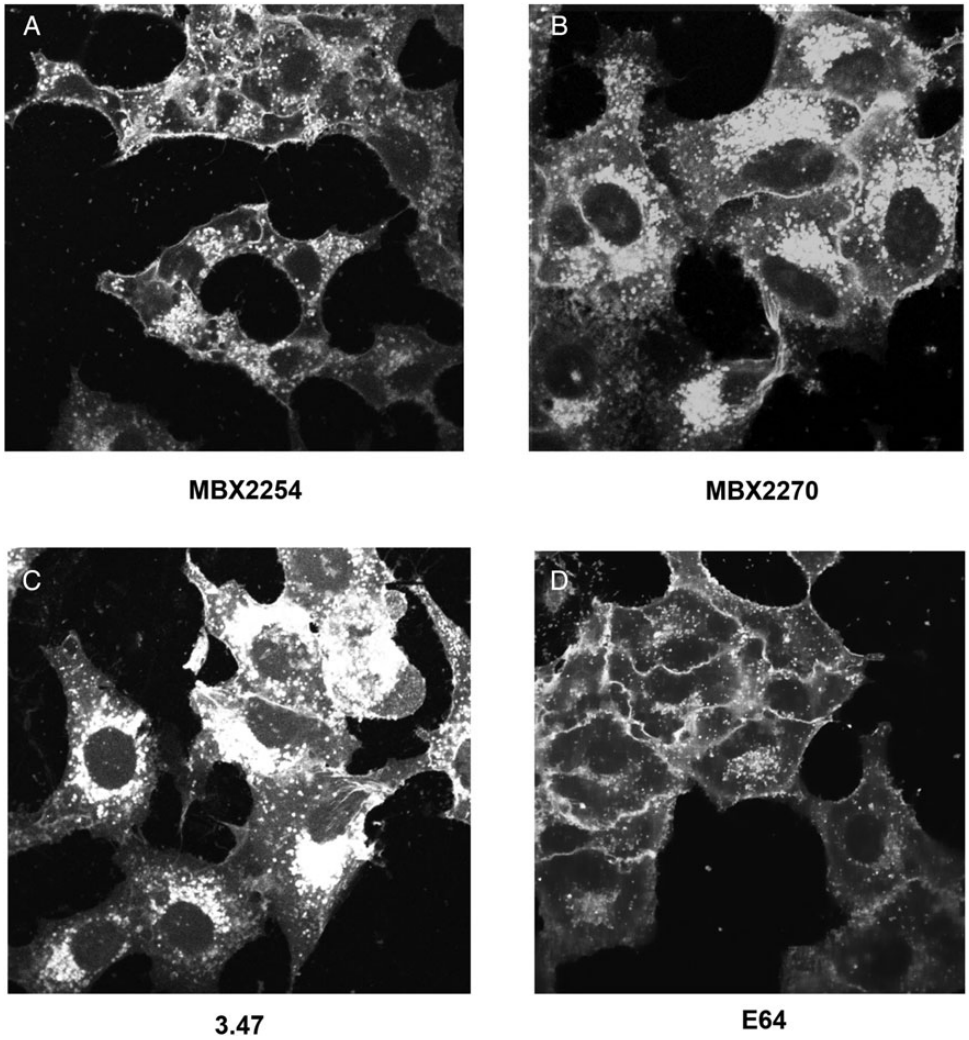


**Figure 4.** MBX2254 and MBX2270 cause cholesterol accumulation in late endosomes/lysosomes. A549 cells were treated for overnight with MBX2254, MBX2270, E64, or compound 3.47 at concentrations described in "Methods" section. Cells were then fixed, stained with filipin, and imaged with a fluorescence microscope. Representative images are shown. Each compound was tested ≥3 times.

binding of thermolysin-cleaved EBOV-GP to NPC1 domain C using an AlphaLISA format (Perkin-Elmer). Protein G–tagged AlphaLISA acceptor beads were coated with thermolysin-cleaved EBOV-GP using the anti-EBOV-GP monoclonal antibody KZ52. Anti-FLAG tagged donor beads were coated with FLAG epitope-tagged NPC1 domain C peptide, as described elsewhere [4]. Compound 3.47, which has been shown to inhibit this interaction, was used as a control. Both MBX2254 and MBX2270 inhibited the interaction of thermolysin-cleaved EBOV-GP with NPC1 domain C in a dose-dependent manner (Figure 5*A*), suggesting that they block EBOV-GP/NPC1 interaction.

To confirm the results, we compared the effects of binding of MBX2254 and MBX2270 on rVSV-GPΔ infection in Chinese hamster ovary cells expressing either basal or higher levels of NPC1. We used the pancaspase inhibitor E64 (functions independent of NPC1) and compound 3.47 (inhibits EBOV-GP/NPC1 domain C interaction) as negative and positive controls, respectively [15, 16]. As shown in Figure 5*B*, higher concentrations of MBX2254, MBX2270 and 3.47 were required to inhibit rVSV-GPΔ in NPC1-overexpressing cells relative to parental cells (Figure 5*B*). In contrast, as expected, E64 inhibited rVSV-GPΔ with the same dose dependence in both parental and NPC1 overexpressing cells (Figure 5*B*).

### Preliminary Structure Activity Relationship Analysis

We compared the pseudotype antiviral data and cytotoxicity measures for several compounds and compared the results with those of the hit compounds, MBX2254 and MBX2270 (Tables 1 and 2, respectively). This preliminary study was designed to explore the effect of electronic properties and steric factors in the

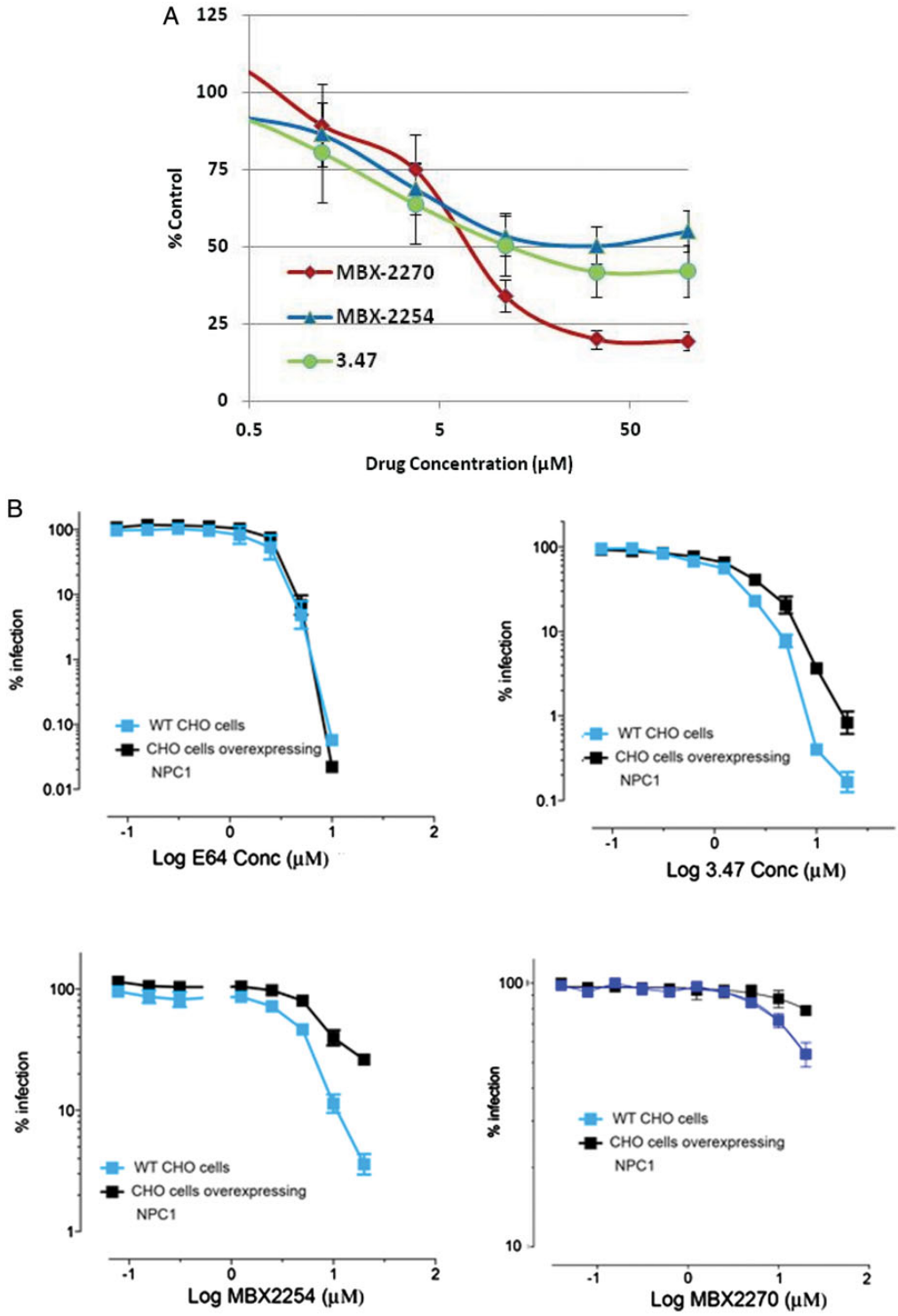


**Figure 5.** MBX2254 and MBX2270 inhibit Ebola virus (EBOV) glycoprotein (GP)/Niemann-Pick C1 (NPC1) domain C interaction. *A*, Effects of MBX2254 and MBX2270 on EBOV GP/NPC1-domain C interaction. The inhibitory effect of compounds MBX2254 and MBX2270 on EBOV GP/NPC1-domain C interaction was investigated in an AlphaLISA format, as described in "Methods" section. Dose-response curves for MBX2254 and MBX2270 are shown. Compound 3.47, which is known to inhibit the EBOV-GP/NPC1-domain C interaction, was used as a positive control. Three independent experiments were performed to determine the effect of compounds. *B*, MBX2254 and MBX2270 inhibit EBOV-GP–mediated infection in an NPC1-dependent manner. Parental wild-type (WT) Chinese hamster ovary (CHO) cells and CHO cells stably overexpressing NPC1 were pretreated with the indicated concentration of inhibitor for 1 hour at 37°C and then infected with rVSV-GPΔ for 18 hours in the continued presence of inhibitor. Each concentration of inhibitor was tested in duplicate. Infection values were normalized to dimethyl sulfoxide–treated samples and averaged across experiments.

**Table 1. Preliminary SAR of Aminoacetamide Sulfonamide Scaffold**

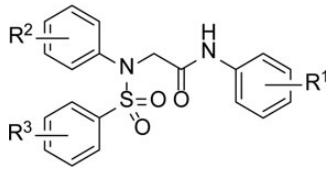

| Compound | $R^1$ | $R^2$ | $R^3$ | HIV/EBOV-GP $IC_{90}$, μmol/L | HIV/EBOV-GP $CC_{50}$, μmol/L | HIV/EBOV-GP SI |
|---|---|---|---|---|---|---|
| MBX2254 | 2-Ph | 4-Me | 4-OMe | 8.6 | >50 | ND |
| 6 175 342 | 4-OMe | 3-OMe | 4-Me | >100 | >100 | ND |
| 6 367 388 | 2,5-diOMe | 2-Cl | 4-Me | 1.6 | 50 | 31 |
| 6 175 402 | 3-Me | 2-Cl | 4-Me | 3.2 | >100 | >31 |
| 5 534 655 | 4-OEt | 4-Me | H | 0.8 | >100 | >125 |
| 6 068 478 | 2-F | 3-Me | H | 0.8 | 50 | 63 |

Abbreviations: $CC_{50}$, 50% cytotoxic concentration; HIV/EBOV-GP, Ebola pseudotype; $IC_{90}$, 90% inhibitory concentration; ND, not determined; SAR, structure activity relationship; SI, selectivity index.

aromatic systems of both inhibitor series on the antiviral activity and cytotoxicity of the compounds. Table 1 shows the results for a few key analogues of MBX2254, 4 active and 1 inactive. We surveyed >50 analogues of the sulfonamide series by either purchasing or synthesizing additional compounds. The result suggests that the system is chemically tractable with some combinations of substituent lowering antiviral activity (Table 1). We also performed preliminary structure activity relationship (SAR) with MBX2270 (Table 2). As with the MBX2254 series, we found that some combinations decrease antiviral activity of MBX2270. Overall, these preliminary SAR results are consistent with a specific target-inhibitor interaction, and the 2 compounds MBX2254 and MBX2270 will be the starting point for further optimization to identify lead compounds using medicinal chemistry.

## DISCUSSION

EBOV-GP controls 2 critical aspects of viral entry: receptor binding and membrane fusion. In this report, we describe 2 small molecules, MBX2254 and MBX2270, based on sulfonamide and triazole thioether scaffolds, respectively, that inhibit EBOV viruses in a potent ($IC_{50}$ of 0.29 to 10 μmol/L) and

**Table 2. Preliminary SAR of Triazole Thioether Scaffold**

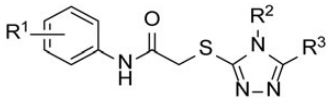

| Compound | $R^1$ | $R^2$ | $R^3$ | HIV/EBOV-GP $IC_{90}$, μmol/L | HIV/EBOV-GP $CC_{50}$, μmol/L | HIV/EBOV-GP SI |
|---|---|---|---|---|---|---|
| MBX2270 | 4-OEt | Ph | 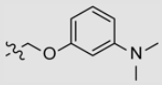 | 25.7 | >50 | ND |
| 7 846 036 | 3-$CF_3$ | Ph | 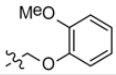 | 6.3 | 55 | 9 |
| 7 629 169 | 2-Cl | Ph | 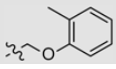 | 2.5 | 21 | 8 |
| 7 909 196 | 2-$CF_3$ | 4-Tol | 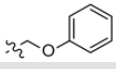 | 82 | >100 | ND |
| 7 682 333 | 3,4-diMe | Et | 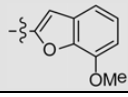 | 6.3 | 35 | 6 |

Abbreviations: $CC_{50}$, 50% cytotoxic concentration; HIV/EBOV-GP, Ebola pseudotype; $IC_{90}$, 90% inhibitory concentration; ND, not determined; SAR, structure activity relationship; SI, selectivity index.

selective 50% cell cytotoxicity concentration ($CC_{50}$) ($CC_{50}$, >50 μmol/L) manner in vitro. Our findings also suggest that the inhibition is due to the ability of MBX2254 and MBX2270 to inhibit EBOV-GP/NPC1 domain C interaction at the late stage of viral entry.

Virus entry is a multistep process, and several approaches were taken to determine the antiviral target. The differential inhibition of HIV/EBOV-GP and HIV/VSV-G by MBX2254 and MBX2270 suggested the specificity of inhibition by the compounds. EBOV entry is mediated in the LE/LYs, whereas VSV viral entry is mediated primarily in early endosomes, soon after internalization [15, 16]. Next we performed "time-of-addition" studies, which indicated that compounds MBX2254 and MBX2270 block viral entry into cells. In addition, compounds MBX2254/MBX2270 inhibited both HIV/EBOV-GP (wild-type) and HIV/EBOV-GPΔmucin with similar potencies (data not shown), suggesting that MBX2254 and MBX2270 do not inhibit the early stage of binding of the virus to the cells surface receptor moieties. In HIV/EBOV-GPΔmucin, the mucin domain is removed to expose the EBOV-GP1 receptor-binding domain.

We further observed (1) cholesterol accumulation on treatment of cells with MBX2254 and MBX2270 (Figure 4*A* and 4*B*); (2) inhibition of the thermolysin-cleaved EBOV-GP and NPC1 domain C interaction (Figure 5*A*); and (3) reduction in MBX2254 and MBX2270 activity in the presence of excess NPC1 (Figure 5*B*). NPC1 binds cholesterol and oxysterols, and the binding site is localized in the luminal loop-1, a 240-amino acid domain and not through domain C of NPC1, the binding site for thermolysin-cleaved EBOV-GP [13, 19, 20]. Compound 3.47, which has been shown to inhibit EBOV-GP/NPC1 binding, also causes cholesterol accumulation [9]. Therefore, together the results suggest that (1) MBX2254 and MBX2270 are inhibiting EBOV-GP/NPC1 interaction and (2) binding of MBX2254 and MBX2270 to NPC1 domain C is inducing a conformational change and blocking cholesterol transport by NPC1. This is supported by the preliminary SAR analysis showing that substitutions at certain positions introduce constraints on the inhibitors and reduce their antiviral activity.

We also investigated the binding of MBX2254 or MBX2270 to purified EBOV-GP, using WaterLOGSY (water ligand observed via gradient spectroscopy) magnetic resonance spectroscopy, which is designed to detect binding of small molecules to high-molecular-mass targets [10]. No binding was detected between MBX2254 or MBX2270 and EBOV-GP at concentrations up to 10 μmol/L (data not shown). However, low solubility of the 2 inhibitors also prevented detection of weak interactions between them. Therefore based on these results, we hypothesize that compounds MBX2254 and MBX2270 inhibit EBOV entry by interacting with a site in the C-loop of NPC1, the binding site for primed EBOV-GP in LE/LYs.

The $IC_{50}$ values of MBX2270 against infectious EBOV were within approximately 2-fold the values for HIV/EBOV-GP, whereas those of MBX2254 against Zaire EBOV were significantly lower (difference, approximately 10-fold). At this time, we do not know the reasons for the differences in $IC_{50}$ values between HIV/EBOV-GP and EBOV-Zaire, but they may be due to differences in the (1) virus shape (EBOV is cylindrical, whereas HIV/EBOV-GP is spherical), (2) EBOV-GP density at the cell surface, (3) EBOV-GP modification (eg, producer cell type-specific glycosylation patterns), or (4) target cells (293T or A549 vs VeroE6). Moreover, the HIV/EBOV-GP contains an HIV core and does not contain the EBOV matrix proteins, VP40 and VP24. However, both VP40 and VP24 play an important role in budding from mammalian cells, and we believe that our compounds do not have any significant effect on VP40 and VP24.

The current West African EBOV outbreak of 2014 is the largest since the virus was discovered in central Africa in 1976. The outbreak also highlights the troubling absence of a direct acting antiviral or vaccine against EBOV to treat infected patients and stop the spread of EBOV. The World Health Organization is currently fast-tracking a trial of several experimental drugs in the hope that they will help reduce the death toll and protect those on the front line of the outbreak. These include ZMapp and TKM-100802. ZMapp is an experimental antibody–based EBOV drug, and convalescent plasma has been administered to 7 infected patients on a case-by-case "compassionate use" basis, however, there have been no formal safety and efficacy studies in humans for ZMapp, and its clinical effectiveness is still uncertain [1, 15]. TKM-100802 is a lipid nanoparticle small interfering RNA–based drug that protects rhesus monkey in a Marburg virus disease model [19].

Others drugs considered for fast-tracking include BCX4430, a broad-spectrum replication inhibitor that protects the cynomolgus macaque in a Marburg virus disease model [21]; T-705 (favipiravir), a substituted pyrazine compound; and adenosine analogue 3-deazaneplanocin A ($c^3$-Npc A). However, T-705 and $c^3$-Npc A do not protect nonhuman primates at the doses they are tested [5, 21–23]; studies with different dosing regimen is currently ongoing. None of the potential EBOV therapies inhibit the EBOV-GP/NPC1 interaction or resembles MBX2254 and MBX2270 structurally. The previously discovered compound 3.47 is going through drug optimization studies [9].

In summary, we have identified 2 novel EBOV inhibitors, MBX2254 and MBX2270, with novel chemical scaffolds that could serve as starting points for the development of therapeutic agents. These results also highlight the importance of the EBOV-GP/NPC1 interaction in EBOV entry and the attractiveness of NPC1 as an antifiloviral therapeutic target. In addition, the compounds can be used as chemical probes for exploring the molecular mechanism of the EBOV-GP/NPC1 interaction in cells.

## Notes

***Acknowledgments.*** We thank Michael Caffrey from the Department of Biochemistry and Molecular Genetics, University of Illinois at Chicago, for

helping us with the WaterLOGSY (water ligand observed via gradient spectroscopy) magnetic resonance spectroscopy. We also thank Richard Adshead from the University of Massachusetts Medical School for helping with fluorescent microscopy.

***Financial support.*** This work was supported by the National Institutes of Health (grants 1R01AI089590 and R01AI101436).

***Potential conflicts of interest.*** All authors: No reported conflicts.

All authors have submitted the ICMJE Form for Disclosure of Potential Conflicts of Interest. Conflicts that the editors consider relevant to the content of the manuscript have been disclosed.

## References

1. Leroy EM, Epelboin A, Mondonge V, et al. Human Ebola outbreak resulting from direct exposure to fruit bats in Luebo, Democratic Republic of Congo, 2007. Vector Borne Zoonotic Dis **2009**; 9:723–8.
2. Ray RB, Basu A, Steele R, et al. Ebola virus glycoprotein-mediated anoikis of primary human cardiac microvascular endothelial cells. Virology **2004**; 321:181–8.
3. Sullivan NJ, Sanchez A, Rollin PE, Yang ZY, Nabel GJ. Development of a preventive vaccine for Ebola virus infection in primates. Nature **2000**; 408:605–9.
4. Misasi J, Sullivan N. Camouflage and misdirection: the full-on assault of Ebola virus disease. Cell **2014**; 159:477–86.
5. Basu A, Li B, Mills DM, et al. Identification of a small-molecule entry inhibitor for filoviruses. J Virol **2011**; 85:3106–19.
6. Takada A, Kawaoka Y. The pathogenesis of Ebola hemorrhagic fever. Trends Microbiol **2001**; 9:506–11.
7. Carette JE, Raaben M, Wong AC, et al. Ebola virus entry requires the cholesterol transporter Niemann-Pick C1. Nature **2011**; 477:340–3.
8. Chandran K, Sullivan NJ, Felbor U, Whelan SP, Cunningham JM. Endosomal proteolysis of the Ebola virus glycoprotein is necessary for infection. Science **2005**; 308:1643–5.
9. Côté M, Misasi J, Ren T, et al. Small molecule inhibitors reveal Niemann-Pick C1 is essential for Ebola virus infection. Nature **2011**; 477:344–8.
10. Basu A, Antanasijevic A, Wang M, et al. New small molecule entry inhibitors targeting hemagglutinin-mediated influenza a virus fusion. J Virol **2014**; 88:1447–60.
11. Manicassamy B, Wang J, Jiang H, Rong L. Comprehensive analysis of Ebola virus GP1 in viral entry. J Virol **2005**; 79:4793–805.
12. Rumschlag-Booms E, Zhang H, Soejarto DD, Fong HH, Rong L. Development of an antiviral screening protocol: one-stone-two-birds. J Antivir Antiretrovir **2011**; 3:8–10.
13. Miller EH, Obernosterer G, Raaben M, et al. Ebola virus entry requires the host-programmed recognition of an intracellular receptor. EMBO J **2012**; 31:1947–60.
14. Zhang JH, Chung TD, Oldenburg KR. A simple statistical parameter for use in evaluation and validation of high throughput screening assays. J Biomol Screen **1999**; 4:67–73.
15. Johansen LM, Brannan JM, Delos SE, et al. FDA-approved selective estrogen receptor modulators inhibit Ebola virus infection. Sci Transl Med **2013**; 5:190ra179.
16. Shoemaker CJ, Schornberg KL, Delos SE, et al. Multiple cationic amphiphiles induce a Niemann-Pick C phenotype and inhibit Ebola virus entry and infection. PLoS One **2013**; 8:e56265.
17. Werle B, Staib A, Julke B, et al. Fluorometric microassays for the determination of cathepsin L and cathepsin S activities in tissue extracts. Biol Chem **1999**; 380:1109–16.
18. Maruyama T, Rodriguez LL, Jahrling PB, et al. Ebola virus can be effectively neutralized by antibody produced in natural human infection. J Virol **1999**; 73:6024–30.
19. Infante RE, Radhakrishnan A, Abi-Mosleh L, et al. Purified NPC1 protein: II. Localization of sterol binding to a 240-amino acid soluble luminal loop. J Biol Chem **2008**; 283:1064–75.
20. Infante RE, Wang ML, Radhakrishnan A, Kwon HJ, Brown MS, Goldstein JL. NPC2 facilitates bidirectional transfer of cholesterol between NPC1 and lipid bilayers, a step in cholesterol egress from lysosomes. Proc Natl Acad Sci U S A **2008**; 105:15287–92.
21. Warren TK, Wells J, Panchal RG, et al. Protection against filovirus diseases by a novel broad-spectrum nucleoside analogue BCX4430. Nature **2014**; 508:402–5.
22. Aman MJ, Kinch MS, Warfield K, et al. Development of a broad-spectrum antiviral with activity against Ebola virus. Antiviral Res **2009**; 83:245–51.
23. Smither SJ, Eastaugh LS, Steward JA, Nelson M, Lenk RP, Lever MS. Post-exposure efficacy of oral T-705 (favipiravir) against inhalational Ebola virus infection in a mouse model. Antiviral Res **2014**; 104:153–5.